Modified Morse potential for unification of the pair interactions

Longjiu Cheng and Jinlong Yang[a)]
Hefei National Laboratory for Physical Sciences at the Microscale, University of Science and Technology of China, Hefei, Anhui 230026, People's Republic of China

(Received 3 July 2007; accepted 6 August 2007; published online 26 September 2007; publisher error corrected 2 October 2007)

We designed a novel model potential that unifies the pair interactions including the well known Morse and Lennard-Jones potentials. Using two parameters, the interactions at the minimum, short range, and long range of the new model potential can be controlled separately, so the potential is very flexible to fit various systems. It is found that for potentials with similar range with the Lennard-Jones potential at the minimum, due to the difference at the short and long ranges, the favorite structures can be very different, and some previously unknown magic numbers are located. © *2007 American Institute of Physics*. [DOI: 10.1063/1.2777148]

I. INTRODUCTION

The energetic and dynamical properties of clusters[1] are often complicated. The electronic structure determines the atomic interactions but for most of the complex systems, quantum mechanics methods are too expensive. Therefore, a simple model and empirical potentials are largely used to fit the interatomic potentials for systematic and overall study of real systems, and the results are generally acceptable in a certain precision.

Pair interaction is the basis of interatomic potentials. The Lennard-Jones (LJ) potential is the most famous one with pair interaction,[2]

$$\mathrm{LJ}(r) = r^{-12} - 2r^{-6}, \tag{1}$$

where r is the pair distance.[3] A LJ potential form can well fit the interactions of rare gas atoms at low temperature and is taken as the van der Waals part for most of the complex empirical and semiempirical forces. Moreover, LJ system often acts as a benchmark problem to check the newly developed theoretical methods. Another well known pair potential is the Morse (M) potential,[4]

$$\mathrm{M}[\rho](r) = e^{2\rho(1-r)} - 2e^{\rho(1-r)}, \tag{2}$$

where ρ is the parameter of the potential, while r is the interatomic distance. At the minimum ($r=1$), the curvature of Morse potential is $\psi=2\rho^2$. Lower values of ψ correspond to a longer potential range. As can be seen from Fig. 1 low values of ρ give a long-ranged potential and high values a short-ranged potential. The potential range is the most important factor for a pair potential determining the favorite structures of clusters; e.g., with ρ increasing, the sequences of global minima of Morse clusters are disordered, core shell, icosahedral, decahedral, and close packed.[5–7] Morse fit is also largely adopted as the pair-interaction part in the many-body potentials.[8,9] Although M[6] and LJ potentials are very different in form, but as shown in Fig. 1, the two potentials have similar shapes with the same curvature at the minimum ($r=1$). The difference is that M[6] is a little softer at the short range ($r<1$) and weaker at the long range ($r>1$).

For Morse potential, with parameter ρ increasing, the potential range at the minimum, long range, and short range decreases at the same time. However, for potentials with similar ranges at the minimum, the favorite global minimum structures may also be very different, which is caused by the difference at the long- and short-range interactions. There is still no systematic study about how the long- and short-range interactions affect the global minimum structures. For this aim, in this work, we try to design a new model pair potential that can freely control the interactions at the minimum, long range, and short range to investigate how the pair interaction affects the global minimum structures.

II. THEORY

A. The modified Morse model potential

Based on the Morse potential, we designed a modified (MM) model potential with two parameters,

$$\mathrm{MM}[\rho,\varphi](r) = (e^{2\rho(1-r^{\varphi})/\varphi} - 2e^{\rho(1-r^{\varphi})/\varphi} - A)/(1+A), \tag{3}$$

where $A=0$ at $\varphi \geqslant 0$ and $A=e^{2\rho/\varphi}-2e^{\rho/\varphi}$ at $\varphi<0$. The new parameter φ can be used to control the long- and short-range interactions. Taking $\rho=6.0$ as a test case, where M[6] potential and LJ potential have the same curvature at the minimum, Fig. 2 plots MM potentials with various values of φ. It can be seen that a larger value of φ will increase the potential range at the short range (or softer) and decrease the potential range at the long range (or weaker), and smaller value of φ will decrease the potential range at the short range (or harder) and increase the potential range at the long range (or stronger). For $\varphi \geqslant 0$, the curvature at the minimum is still $\psi=2\rho^2$, where the potential range at the minimum does not change with φ; i.e., MM potential has the same potential range at the minimum with the Morse potential. For $\varphi<0$, the curvature at the minimum becomes $\psi=2\rho^2/(1-e^{\rho/\varphi})^2$, where the potential range at the minimum decreases. How-

[a)]Author to whom correspondence should be addressed. Tel.: +86-551-3606408; Fax: +86-551-3602969. Electronic mail: jlyang@ustc.edu.cn

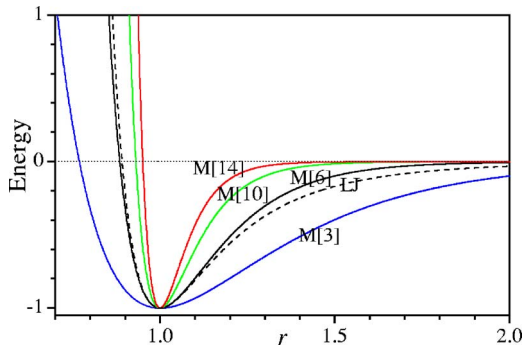

FIG. 1. (Color online). Plots of the LJ and the Morse potentials for different values of ρ (as labeled).

ever, as can be seen from Fig. 2, when φ is not too negative, the change of the potential range at the minimum is very small.

Obviously, MM potential is just the Morse potential at $\varphi=1$. Interestingly, by chance, we found that when $\rho=6$ and $\varphi\to 0$,

$$\lim_{\varphi\to 0} e^{(1-r^{\varphi})/\varphi} = r^{-1} \Rightarrow \mathrm{MM}[6,\varphi\to 0](r) = r^{-12} - 2r^{-6} = \mathrm{LJ}(r), \quad (4)$$

where MM potential is the LJ potential. Thus, the MM potential unifies the two famous pair potentials. When $\varphi>0$, similar to the Morse potential, at $r\to 0$, the value of MM potential is a positive number $(e^{2\rho/\varphi}-2e^{\rho/\varphi})$ instead of $+\infty$. However, if the value is large enough, the potential is still reasonable for simulations. The value of MM potential is -1 at $r=1$ and 0 at $r\to+\infty$, so the potential is given in the standard form.

Using two parameters, MM potential is very flexible in controlling the potential range at the short range, minimum, and long range. Figure 2 has shown that potentials with similar ranges at the minimum but with various short- and long-range interactions can be modeled by MM potentials. Moreover, as shown in Fig. 3, potentials with similar long-range interactions and various short-range interactions and potentials with similar short-range interactions and various long-range interactions can also be well fitted. Therefore, we can expect that the MM potential is better than (at least not worse than) the Morse potential in fitting the bonded or nonbonded interactions for various systems in the many-body empirical potentials.

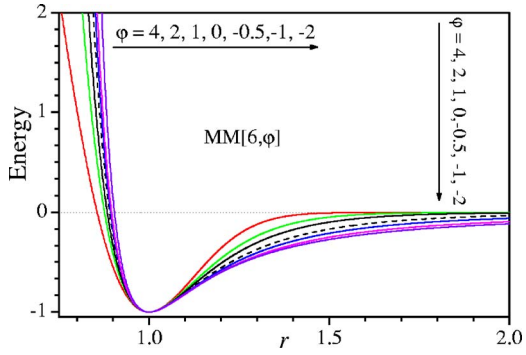

FIG. 2. (Color online). Plots of the modified Morse potentials for $\rho=6$ and different values of φ (as labeled).

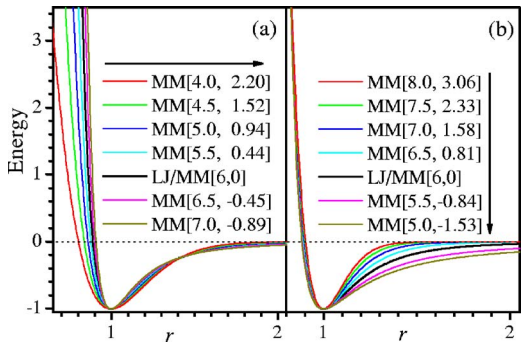

FIG. 3. (Color online). Plots of (a) MM potentials with similar long-range interactions ($r>1$) and various short-range interactions ($r<1$) and (b) MM potentials with similar short-range interactions and various long-range interactions. For each case, parameter ρ is given and parameter φ is obtained by fitting the long- and short-range interactions of LJ potential, respectively.

B. Global optimization method

To locate the putative global minimum structures of MM clusters, the dynamic lattice searching (DLS) method is used for global optimization, which is an unbiased cluster optimization method that combines the advantages of the lattice searching method and the stochastic unbiased global optimization method and has been proven to be very efficient for cluster systems.[10,11]

III. RESULTS AND DISCUSSION

A. Global minima of MM[6,−2] and MM[6,4] clusters

Now, using different MM potentials as examples, we will illustrate how the long- and short-range interactions affect the global minimum structures of clusters. The LJ (MM[6,0]) and Morse (MM[ρ,1]) clusters have been systematically studied in literature.[12] LJ and M[6] potentials are both middle ranged, where at small cluster sizes, icosahedral structures are predominant in potential energy, and only at some magic numbers, decahedral or face-centered cubic (fcc) structures can be global minimum. To have easy comparisons, we select MM[6,−2], a potential with stronger long-range interaction and harder short-range interaction, and MM[6,4], a potential with weaker long-range interaction and softer short-range interaction, as test cases to compare their favorite structures. Using the DLS method, we located the putative global minimum structures of MM[6,−2] and MM[6,4] clusters up to cluster size $N=210$.[13]

The energies of the resulting putative global minima of MM[6,−2] and MM[6,4] clusters are depicted in Fig. 4 in a manner that emphasizes particular stable minima or "magic numbers." The icosahedral magic numbers ($N=13$, 19, 23, 26, 55, and 147) are plotted in Fig. 5(a), where 13, 55, and 147 are regular Mackay icosahedra (Ihs): Ih13, Ih55, and Ih147, respectively. 19, 23, and 26 are Ih13 plus various regular anti-Mackay overlayers (Ih+) but can also be taken as Ih13-based poly-Ihs (pIhs): line, triangle, and pyramid, respectively. The icosahedral magic numbers are known as

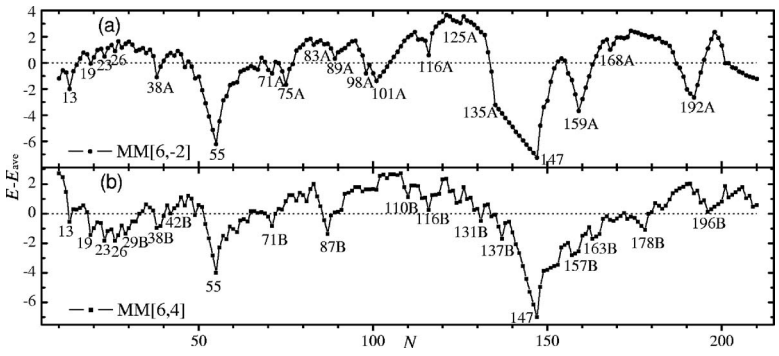

FIG. 4. Energy of the global minima of (a) MM[6,−2] and (b) MM[6,4] clusters relative to E_{av}, a fit to the energies of the global minima at size ratio of $10 \leqslant N \leqslant 210$ using the form $a+bN^{1/3}+cN^{2/3}+dN$, which represents the average energy of the global minima.

particularly stable structures of LJ clusters, and as can be seen from Figs. 4(a) and 4(b), they also act as particularly stable structures for MM[6,−2] and MM[6,4] clusters because the three potentials have similar ranges at the minimum. However, due to the difference at the short and long ranges of the potentials, there are also some very novel magic numbers for MM[6,−2] and MM[6,4] clusters compared to LJ or M[6] clusters.

The hardness at the short range makes MM[6,−2] potential disfavor the strain of $r<1$, and the strong long-range interaction makes the potential favor more spherical clusters compared to the number of nearest neighbors (NN), so the magic numbers of fcc, close-packed, tetrahedral, and decahedral clusters can act as the particularly stable structures. Figure 5(b) plots the particularly stable or novel global minima of MM[6,−2] clusters: 38A is the magic number of fcc cluster, 37A is a close-packed cluster with one {111} surface layer different from 38A, 116A is a truncated fcc tetrahedron plus antilayers outside the four {111} surfaces, and 125A is 116A plus a cap; 75A, 101A, and 192A are regular Marks decahedrons,[14] and 71A is 75A minus four patch atoms; 34A, 98A, and 159A, are the Leary tetrahedronlike[15] clusters (based on the three-, four-, and five-atom edged tetrahedrons, respectively), 89A is 98A minus a cap, and 168A is 159A plus a cap; and 83A is one {111} face (six atoms) missed Ih55 plus Mackay overlayers, 86A is one {111} face (three atoms) missed Ih13 plus three levels of Mackay overlayers, and 135A is the 12-vertices missed Ih147. Interestingly, the Leary tetrahedral 89A can also be seen as an icosahedral one similar to 86A but the last layer is an anti-Mackay one, and 92A is 89A plus three atoms to complete the Ih13 core. The similarity of 86A and 89A may be helpful to learn the relationship between icosahedral and Leary tetrahedral clusters. The incompleteness of the icosahedral core will decrease the number of NN but can also decrease the strain energy. 38A, 75A, and 192A are also the global minima for LJ clusters but are not particularly stable compared to the neighbors.

Due to the weakness at the long range, MM[6,4] potential disfavors the strain of $r>1$ and the number of NN is much more important than sphericity. Moreover, the softness at the short range can reduce the strain energy of $r<1$. Therefore, besides the icosahedral magic numbers, some novel pIh magic numbers, which are less spherical but have more NN and are less strained of $r>1$, also act as the particularly stable structures. Figure 5(c) plots the particularly stable or novel global minima of MM[6,4] clusters: 25B, 29B, and 34B are Ih13-based pIh structures similar to 19, 23, and 26; 38B is pIh in a sixfold manner,[16,17] 40B is 38B plus two atoms in the sixfold tips, and 42B is 38B plus four atoms to form another Ih13 sharing one edge of 38B; 87B and 110B are Ih55-based pIh with similar mechanisms to 19 and 23, respectively; 190B is Ih147-based incomplete pIh; 71B is Ih55 plus a regular antilayer cap; 116B, 131B, 137B, and 141B are Ih55 plus various incomplete Mackay outer shells; 157B, 163B, and 178B are Ih147 plus various anti-Mackay caps; and 196B is Ih147 plus regular Mackay overlayers. For some Ih13-based cases (19, 23, 26, 25B, and 29B), the pIh motif can also be thought as Ih plus anti-Mackay overlayers (Ih+). For the Ih55- or Ih147-based cases, there are also relationships between Ih+ and pIh motifs, e.g., 87B is 71B

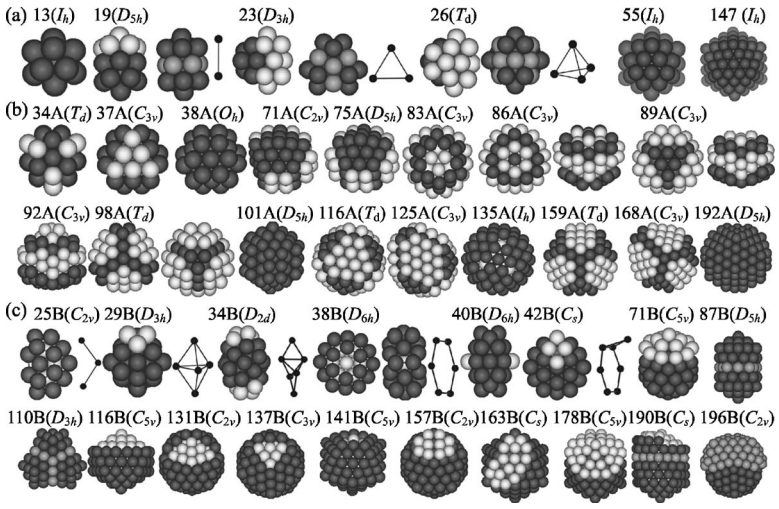

FIG. 5. Structures of (a) the icosahedral magic numbers, (b) most stable or typical global minima of MM[6,−2] clusters, and (c) most stable or typical global minima of MM[6,4] clusters. For some cases, two sides of views are given, and the sites are given in different shades to show the topological structure more clearly. The dot-line model gives the pattern of pIh.

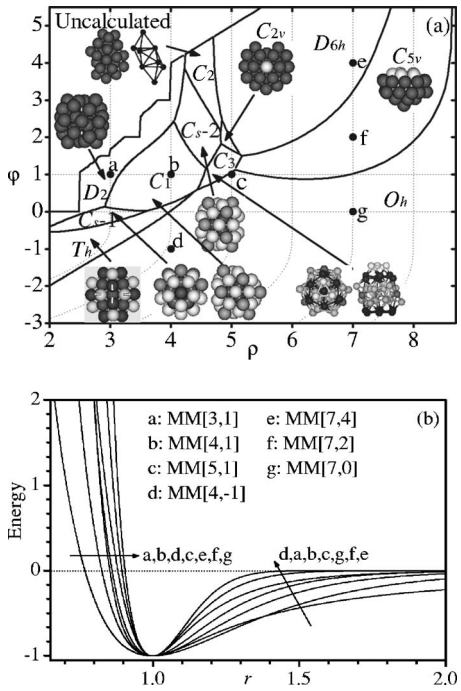

FIG. 6. (a) Structural phase diagram of MM_{38} cluster showing how the structure of the global minimum depends on ρ and φ. The horizontal grid lines give $\varphi=1$ (Morse potential) and 0, and the vertical grid lines represent the same potential range at the minimum. (b) The potentials of the points are marked in (a).

plus another 16-atom cap on the anti-Mackay cap and 190B is 178B plus overlayers on the anti-Mackay cap.

B. Structural phase diagram of MM_{38}

The difference of the global minima of MM[6,−2] and MM[6,4] clusters shows that the short- and long-range interactions can greatly affect the global minimum structures for potentials with similar ranges at the minimum. Finally, to give an overall view of how the global minimum structures depend on ρ and φ, we locate the global minimum structures of MM_{38} cluster as a function of ρ and φ and plot the structural phase diagram showing the variation of the lowest-energy structure with ρ and φ in Fig. 6(a). The shape of the MM potentials at some selected points is plotted in Fig. 6(b).

First, at very small value of ρ (very long ranged), the global minimum (D_2) is an amorphous structure, which is most compact and strained, and has the largest number of NN. Second, with ρ increasing or φ decreasing, Ih13-based pIh structures (C_s-1, C_1, C_s-2, and C_2) become global minima, which are less strained or more spherical. In the four pIh structures, C_s-1 is the most spherical but has the least number of NN, so it is more favored at smaller φ, where the interaction at the long range is stronger; however, C_2 is not spherical but is less strained for $r>1$, so it is more favored at a larger φ. Then, at large φ, with ρ increasing, the strain energy of $r>1$ grows more rapidly than that of $r<1$, so the sixfold Ih13-based pIh structures (D_{6h} and C_{2v}), which are more strained for $r<1$ but less strained for $r>1$,[18] become global minima. C_{2v} is different from D_{6h} (38B) by moving two edge atoms to the sixfold tips, which has more NN and is more spherical but is more strained for $r>1$ than D_{6h}, and so is more dominant at small ρ and φ. Next, with ρ increasing or φ decreasing, the strain energy of $r<1$ is also too large for the sixfold pIh structures, so the icosahedral structure (C_{5v}) that has less NN but is less strained becomes the global minimum. Lastly, with ρ increasing or φ decreasing, C_{5v} also becomes too strained, so the strain-free fcc structure (O_h) that has less NN and is spherical becomes the global minimum. O_h (38A) is the most spherical, so it is predominant at small φ even for very small ρ. T_h is a slight distortion of O_h, where the six {100} faces are distorted to {111} faces to have more NN. C_3 is a surprise disordered structure at such potential range,[7] which has a similar packing style of the recently located chiral global minimum of Au_{34}^- cluster[19] that can be seen as a serious distortion of a close-packed structure.

IV. CONCLUSION

In summary, we designed novel MM model pair potentials that can freely control the interactions at the minimum, short range, and long range of the potential by using two parameters ρ and φ. For $\varphi=1$, MM potential is the Morse potential, and for $\rho=6$ and $\varphi\to 0$, MM potential is the LJ potential, where the two famous pair potentials are unified. By comparing the global minimum structures of LJ potential, MM[6,−2] potential, and MM[6,4] potential, where the three potentials are both middle ranged at the minimum but are different at the short and long ranges, it is found that the particularly stable structures can be very different at some magic numbers. The structural phase diagram of MM_{38} cluster is also given to have an overall view of how the global minimum structures depend on ρ and φ. In the test calculations, some novel structures are located as magic numbers, which are previously unknown but may be global minimum structures for certain real systems.

The potential application of MM potential is to fit the bonded or nonbonded interactions for various systems (e.g., liquids, metal clusters, and molecular clusters) in the many-body empirical potentials. Besides the values of the pair well depth and the equilibrium pair distance (or bond length), due to the large-scale flexibility, MM potential should be better in fitting the data of some real systems compared to other potential forms. Another potential application of MM potentials is to act as a model potential to investigate how the pair potential affects the global minimum structures, phase transition temperatures, thermodynamic properties, kinetic properties, etc., which may be helpful to grasp the physical essences out of the complicated behaviors of real systems. Moreover, MM potentials can be used to investigate how the short- and long-range interactions affect the potential energy surface of clusters, adding to the work of Wales, where the Morse potential was adopted to study the relationship of the range of the pair interaction and the potential energy surface using the catastrophe theory.[20]

ACKNOWLEDGMENTS

This work is partially supported by the National Natural Science Foundation of China (Nos. 50121202, 20533030, and 10474087), by the National Basic Research Program of

China (No. 2006CB922004), by the K. C. Wong Education Foundation, Hong Kong, by the China Postdoctoral Science Foundation (CPSF), by the USTC-HP HPC Project, and by the SCCAS and Shanghai Supercomputing Center. The authors acknowledge Dr. Xie for a helpful discussion.

[1] F. Baletto and R. Ferrando, Rev. Mod. Phys. **77**, 371 (2005).
[2] J. E. Lennard-Jones, Proc. R. Soc. London, Ser. A **109**, 584 (1925).
[3] In this paper, as a benchmark study, we set the pair well depth as the unit of the energy ($\varepsilon=1$) and the equilibrium pair distance as the unit of the distance ($r_0=1$).
[4] P. M. Morse, Phys. Rev. **34**, 57 (1929).
[5] J. P. K. Doye, D. J. Wales, and R. S. Berry, J. Chem. Phys. **103**, 4234 (1995).
[6] J. P. K. Doye and D. J. Wales, J. Chem. Soc., Faraday Trans. **93**, 4233 (1997).
[7] L. J. Cheng and J. L. Yang, J. Phys. Chem. A **111**, 5287 (2007).
[8] M. Quack and M. A. Suhm, J. Chem. Phys. **95**, 28 (1991).
[9] J. M. Pacheco and J. P. Prates-Ramalho, Phys. Rev. Lett. **79**, 3873 (1997).
[10] X. G. Shao, L. J. Cheng, and W. S. Cai, J. Comput. Chem. **25**, 1693 (2004).
[11] L. J. Cheng, W. S. Cai, and X. G. Shao, ChemPhysChem **8**, 569 (2007).
[12] Cambridge Cluster Database (CCD) (http://www-wales.ch.cam.ac.uk/CCD.html).
[13] Coordinates of the global minima and the table along with the energies, motifs, point groups, number of nearest neighbors, and strain energies are available from the webpage (http://staff.ustc.edu.cn/~clj/modified_morse/table.html).
[14] L. D. Marks, Philos. Mag. A **49**, 81 (1984).
[15] R. H. Leary and J. P. K. Doye, Phys. Rev. E **60**, R6320 (1999).
[16] J. P. K. Doye, D. J. Wales, and S. I. Simdyankin, Faraday Discuss. **118**, 159 (2001).
[17] G. Rossi, A. Rapallo, C. Mottet, A. Fortunelli, F. Baletto, and R. Ferrando, Phys. Rev. Lett. **93**, 105503 (2004).
[18] J. P. K. Doye and D. J. Wales, Phys. Rev. Lett. **86**, 5719 (2001).
[19] A. Lechken, D. Schooss, J. R. Stairs, M. N. Blom, F. Furche, N. Morgner, O. Kostko, B. von Issendorff, and M. M. Kappes, Angew. Chem., Int. Ed. **46**, 1 (2007).
[20] D. J. Wales, Science **293**, 2067 (2001).